



Delft University of Technology

Mean-field dynamics of the non-consensus opinion model

Liu, Xinhan; Achterberg, M. A.; Kooij, Robert

DOI

[10.1007/s41109-024-00656-w](https://doi.org/10.1007/s41109-024-00656-w)

Publication date

2024

Document Version

Final published version

Published in

Applied Network Science

Citation (APA)

Liu, X., Achterberg, M. A., & Kooij, R. (2024). Mean-field dynamics of the non-consensus opinion model. *Applied Network Science*, 9(1), Article 47. <https://doi.org/10.1007/s41109-024-00656-w>

Important note

To cite this publication, please use the final published version (if applicable). Please check the document version above.

Copyright

Other than for strictly personal use, it is not permitted to download, forward or distribute the text or part of it, without the consent of the author(s) and/or copyright holder(s), unless the work is under an open content license such as Creative Commons.

Takedown policy

Please contact us and provide details if you believe this document breaches copyrights. We will remove access to the work immediately and investigate your claim.

RESEARCH

Open Access



Mean-field dynamics of the non-consensus opinion model

Xinhan Liu^{1*}, M. A. Achterberg² and Robert Kooij^{1,2}

*Correspondence:
x.liu-22@tudelft.nl

¹ Faculty of Electrical Engineering, Mathematics and Computer Science, Delft University of Technology, P.O. Box 5031, 2600, GA, Delft, The Netherlands

² Unit ICT, Strategy & Policy, TNO, The Hague, The Netherlands

Abstract

In 2009, Shao et al. (Phys Rev Lett 103(1):018701, 2009) introduced the Non-consensus opinion (NCO) model, which allows different opinions to coexist in the steady state. We propose a mean-field-based dynamical model for the NCO model on networks with low degree correlation, which reveals the mechanism of opinion formation in the NCO model. This mean-field model provides a new way of estimating important system properties such as the fraction of a certain opinion F , the critical threshold f_c , and the size of the largest connected cluster for a given opinion s_1 . It offers an accurate estimation in less time than the Monte Carlo simulations. The scale invariance of the NCO model is discussed. The variation in the degree of nodes holding different opinions in the dynamics of the NCO model is investigated. The trends in the dynamics of the NCO model are also revealed. This approach can be applied to real-world social networks, providing a method of analyzing opinion dynamics in human society.

Introduction

In recent years, there has been significant progress in the study of social dynamics and group behavior, with particular focus on the dissemination of opinions within social networks (Aletti et al. 2010; Sirbu et al. 2016; Sun et al. 2013; Hassani et al. 2022). Opinion dynamics is driven by human behavior and is dependent on many factors, including individual predisposition, the influence of other people (social networks playing a crucial role in this respect), and many others. Different models have been developed, encompassing different elements of the opinion formation process. The study of opinion dynamics was first undertaken by John R. P. et al. in 1956 French (1956). Several models of opinion dynamics with varying rules for forming opinions have emerged over the past decades, including the Galam model (Galam et al. 1982; Galam 2008), Sznajd model (Sznajd-Weron and Sznajd 2000; Katarzyna Sznajd-Weron 2005), the voter model (Lambiotte and Redner 2008; Shang 2018; Redner 2019), the majority rule model (Galam 2002), and, Deffuant model (Shang 2013). These models explore the evolution of competing opinions, which can be mapped to spin models and find applications in the fields of physics, biology, chemistry and social science.

Most spin-type opinion models tend to converge to a consensus state with a single opinion, which does not fully reflect the coexistence of different opinions observed in real life.

To address this, Shao et al. introduced a non-consensus opinion model (NCO model) that allows for a stable coexistence state (Shao et al. 2009). Shao et al. discovered that the opinion formation process in the NCO model can be mapped to a percolation problem, which is characterized by the appearance of a large spanning cluster of the minority opinion. This was the first time that a social dynamic model was mapped to percolation (Li et al. 2013).

In the NCO model, when the fraction of nodes holding a particular opinion surpasses a critical threshold, these nodes form a supportive cluster, where each member receives sufficient backing from others within the cluster. This phenomenon mirrors real-life scenarios where certain groups in society uphold extreme opinions that contradict the majority view, yet they persist due to the cohesive support they receive from like-minded individuals. Consequently, these extreme opinions are challenging to eradicate.

Other researchers have extended the NCO model in various directions. Li et al. (2011) proposed the Inflexible Contrarian Opinion (ICO) model, which introduces stubborn nodes that consistently maintain their opinions, regardless of the opinion of their neighbours. Li et al. (2013) incorporated a weight factor w for each node in the NCO model, giving rise to the NCO w model. Liu et al. (2023) extend the NCO model by introducing three types of malicious nodes, that intend to interfere with the NCO dynamics. Ben-Avraham (2011) develops exact solutions of the NCO model in one dimension and in a Cayley tree. These advancements have provided valuable insights into understanding the dynamics of opinion formation and coexistence in complex social networks.

However, a theory explaining the dynamics of the NCO model has been lacking. The main contribution of this paper is the proposal of a mean-field-based theory for the NCO model, along with a series of governing equations used to analyze its dynamics. The mean-field-based theory of the NCO model can be used to estimate important system properties, such as the opinion fraction of a certain opinion, the size of the largest connected component, and the critical threshold. Compared to Monte Carlo simulations, the mean-field method is both accurate and more efficient. The mean-field description offers an analytical approach of studying the behavior of the NCO model. In this paper, we first introduce the basic opinion formation rules of the NCO model and discuss important parameters of interest in “[The NCO model](#)” section. In “[Mean-field dynamics of NCO model](#)” section, the core of this paper, the mean-field dynamics of the NCO model are presented. The mean-field-based NCO-governing equations are also presented in this section. In “[Simulation results and discussions](#)” section, we explain how to use the mean-field-based NCO governing equations to compute the opinion fraction, the size of the largest connected component, and the critical threshold, and compare them with simulation results. The results obtained from the mean-field-based NCO governing equations show high accuracy, indicating that the mean-field theory accurately explains opinion formation in the NCO model. The degree variation and behavioral trends in the NCO model are also discussed. In “[Conclusion](#)” section summarizes the paper.

The NCO model

The NCO model describes the opinion formation process of two distinct opinions, labeled as σ_+ and σ_- , within a network, where each node adopts one of these two opinions. The network $G(V, E)$ consists of the set V of nodes, representing individual agents,

and the set E of links represent the social connections between the agents. The neighborhood of each node v is denoted as \mathcal{N}_v , encompassing all nodes adjacent to v .

The dynamics of the NCO model are demonstrated in Fig. 1. At each discrete time step t , nodes determine their opinion state $S_v(t)$ (either +1 or -1) based on their own opinion and the opinions of their neighbours. If a node’s local majority opinion aligns with its own, it will keep its current opinion. Conversely, if the local majority opinion differs, the node will change its opinion. This process is represented by the following equation:

$$S_v(t) = \text{sign} \left((1 + \varepsilon) \cdot S_v(t - 1) + \sum_{u \in \mathcal{N}_v} S_u(t - 1) \right) \tag{1}$$

where \mathcal{N}_v represents the set of neighboring nodes of vertex $v \in V$, and $\varepsilon \in (0, 1)$ is a parameter that ensures nodes keep their own opinion when a local majority opinion does not exist.

A crucial parameter of the NCO model is the opinion fraction $F(t)$, which is defined as the proportion of nodes holding the σ_- opinion at a certain time t :

$$F(t) = \frac{n_{\sigma_-}(t)}{N} \tag{2}$$

where $n_{\sigma_-}(t)$ is the number of nodes holding the σ_- opinion at time t , and N is the total number of nodes in the system.

At the beginning, the two opinions σ_- and σ_+ are randomly distributed in the network, with a fraction f and $1 - f$, respectively. Figure 2a shows how the opinion fraction $F(t)$ changes with $f = 0.3$ over time t . When the σ_- opinion is a minority opinion ($f < 0.5$), F decreases with time t according to the dynamics rule of the NCO model. However, the value of F does not go to zero, which is what distinguishes the non-consensus model from other spin-type models.

Figure 2b shows the final opinion fraction F , normalized size of the largest σ_- cluster s_1 and normalized size of the second largest σ_- cluster s_2 for an Erdős–Rényi (ER) graph with $N = 10,000$ nodes and average degree 4. It is conceivable that steady-state opinion fraction F increases with initial opinion fraction f . Shao et al. found that the NCO model in random networks exhibits a second-order phase transition that belongs to regular mean-field percolation. There exists a critical threshold f_c , below which the relative size of the largest cluster s_1 tends to 0. Once the initial opinion fraction f is larger than f_c , a

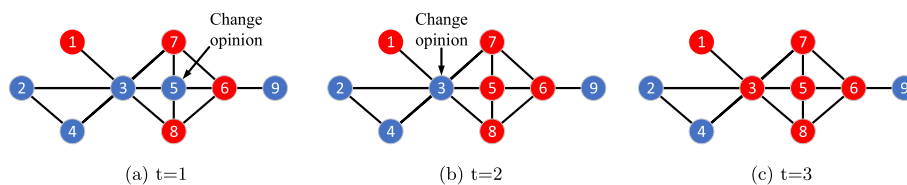


Fig. 1 Dynamics of the NCO model on a network with $N = 9$ nodes. **a** At $t = 0$, 4 nodes are assigned with a σ_+ opinion (red), and the other 5 nodes with a σ_- opinion (blue). This makes node 5 to judge its local opinion ratio as $\sigma_+ : \sigma_- = 3:2$. Node 5 converts to σ_+ . **b** At $t = 1$, node 3 judges its local opinion ratio as $\sigma_+ : \sigma_- = 3:2$ and node 6 converts to σ_+ . **c** At $t = 2$, all nodes hold an opinion that they consider to be a local majority. Hence, the network has reached a steady state

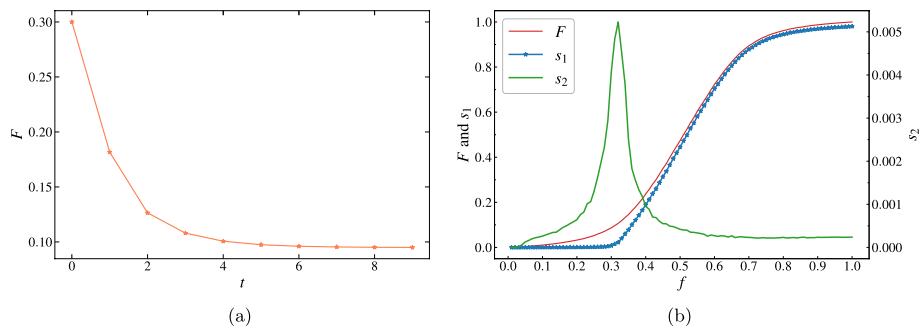


Fig. 2 **a** The fraction of σ_- opinion as a function of time t for an ER network with $N = 10,000$, $p = 0.0004$, and initial opinion fraction $f = 0.03$. **b** Normalized size of the largest cluster s_1 (blue line), the second largest cluster s_2 (green full line) and the fraction of σ_- nodes F (red full line) in the steady state for an ER network with $N = 10,000$ and $p = 0.0004$

giant component emerges in the steady state, which is accompanied by a peak in the relative size of the second-largest cluster s_2 . For the situation in Fig. 2b, the critical threshold f_c roughly occurs at $f_c \approx 0.28$.

Mean-field dynamics of NCO model

Past research on non-consensus models has primarily been conducted through simulations. These models require calculating the state of each node at the next iteration step based on the states of its neighbors. Here, we introduce a dynamics model based on the mean field approach for the NCO model, which offers another angle for understanding and analyzing the NCO model. The mean-field dynamics of the NCO model can provide deeper insights into the system’s behavior. The mean-field dynamics of the NCO model is based on the assumption that each node in the network selects its interacting neighbors without any preference, which means that the network does not have any degree–degree correlation (or a very low degree–degree correlation). In this model, we define the state of a node by its current opinion and by counting its σ_- and σ_+ neighbors. We then use the fractions of nodes in different states to represent the system’s state as, $s = \{f_{\sigma_-,0,0}, \dots, f_{\sigma_-,i,j}, \dots\}$. The mean-field dynamics of NCO model investigates the evolution of these fractions.

The basic idea of the Mean-Field-NCO model is that when nodes in the system change their opinions, the opinions of all their neighbors change with the same probability. According to the fraction of nodes that change the opinions, we can compute the probability that the neighbors of nodes in the system changes their opinions. According to this probability, fractions of nodes with composition of neighboring nodes at next time slot are obtained.

We regard networks of nodes holding the same opinion in the system as a subgraph. There are two subgraphs in the network, the σ_- subgraph and the σ_+ subgraph, as shown in the example in Fig. 3.

Instead of considering the state of every node independently, we aggregate nodes holding the same opinion with the same composition of neighboring nodes. Let f_{σ_-} and f_{σ_+} denote the fractions of nodes holding σ_- and σ_+ opinions, respectively. At time $t = 0$, in both the σ_- and σ_+ subgraphs the fraction of nodes that have d_{σ_-} σ_- neighbors and d_{σ_+} σ_+ neighbors is given by:

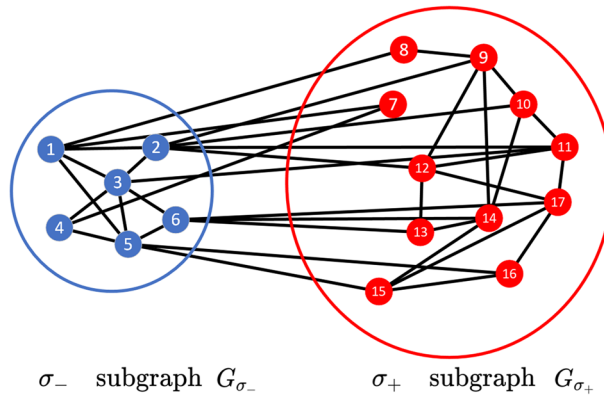


Fig. 3 State of a NCO system at certain time slot t . A graph with 17 nodes, which 6 nodes holding the σ_- opinion and 11 nodes holding the σ_+ opinion. The graph G_{σ_-} consists of the σ_- subgraph and the graph G_{σ_+} consists of the σ_+ subgraph

$$\begin{aligned}
 f_{\sigma_-,d_{\sigma_-},d_{\sigma_+}}(t=0) &= f_{\sigma_-} \cdot \theta_{k=d_{\sigma_-}+d_{\sigma_+}} \cdot \binom{d_{\sigma_-}+d_{\sigma_+}}{d_{\sigma_-}} \cdot f_{\sigma_-}^{d_{\sigma_-}} \cdot f_{\sigma_+}^{d_{\sigma_+}} \\
 f_{\sigma_+,d_{\sigma_-},d_{\sigma_+}}(t=0) &= f_{\sigma_+} \cdot \theta_{k=d_{\sigma_-}+d_{\sigma_+}} \cdot \binom{d_{\sigma_-}+d_{\sigma_+}}{d_{\sigma_-}} \cdot f_{\sigma_-}^{d_{\sigma_-}} \cdot f_{\sigma_+}^{d_{\sigma_+}}
 \end{aligned}
 \tag{3}$$

where θ_k represents the fraction of nodes with degree k , and $\binom{d_{\sigma_-}+d_{\sigma_+}}{d_{\sigma_-}}$ denotes a binomial coefficient.

According to the opinion formation rule of the NCO model, a σ_- (σ_+) node with more neighbors holding a different opinion with them than neighbors holding the same plus one (the node’s own opinion) will change its opinion. As the opinions of σ_- (σ_+) nodes change, the number of links in σ_- (σ_+) nodes will also change. We denote the sets of nodes that change their opinion from σ_- to σ_+ and from σ_+ to σ_- as S_{σ_+} and S_{σ_-} , like the example in Fig. 4 shows. The fraction of nodes with different composition of neighboring nodes in sets $G_{\sigma_-} \setminus S_{\sigma_+}$, $G_{\sigma_+} \setminus S_{\sigma_-}$, S_{σ_-} , and S_{σ_+} are denoted as $f'_{\sigma_-,d_{\sigma_-},d_{\sigma_+}}$, $f'_{\sigma_+,d_{\sigma_-},d_{\sigma_+}}$, $f''_{\sigma_-,d_{\sigma_-},d_{\sigma_+}}$, and $f''_{\sigma_+,d_{\sigma_-},d_{\sigma_+}}$, respectively, where

$$\begin{aligned}
 G_{\sigma_-} : d_{\sigma_+} > d_{\sigma_-} + 1 : f'_{\sigma_-,d_{\sigma_-},d_{\sigma_+}} &= 0, & f''_{\sigma_+,d_{\sigma_-},d_{\sigma_+}} &= f_{\sigma_-,d_{\sigma_-},d_{\sigma_+}} \\
 G_{\sigma_+} : d_{\sigma_-} > d_{\sigma_+} + 1 : f'_{\sigma_+,d_{\sigma_-},d_{\sigma_+}} &= 0, & f''_{\sigma_-,d_{\sigma_-},d_{\sigma_+}} &= f_{\sigma_+,d_{\sigma_-},d_{\sigma_+}} \\
 G_{\sigma_-} : d_{\sigma_+} \leq d_{\sigma_-} + 1 : f'_{\sigma_-,d_{\sigma_-},d_{\sigma_+}} &= f_{\sigma_-,d_{\sigma_-},d_{\sigma_+}}, & f''_{\sigma_+,d_{\sigma_-},d_{\sigma_+}} &= 0 \\
 G_{\sigma_+} : d_{\sigma_-} \leq d_{\sigma_+} + 1 : f'_{\sigma_+,d_{\sigma_-},d_{\sigma_+}} &= f_{\sigma_+,d_{\sigma_-},d_{\sigma_+}}, & f''_{\sigma_-,d_{\sigma_-},d_{\sigma_+}} &= 0
 \end{aligned}
 \tag{4}$$

In the G_{σ_-} and G_{σ_+} subgraphs, the process of nodes changing their opinions involves removing some nodes and links, while adding new ones. For both subgraphs, the fractions of links that fail are described as follows:

$$f_{\sigma_-fail} = \frac{\sum f''_{\sigma_+,d_{\sigma_-},d_{\sigma_+}} \cdot d_{\sigma_-}}{\sum f_{\sigma_-,d_{\sigma_-},d_{\sigma_+}} \cdot d_{\sigma_-}}
 \tag{5}$$

and

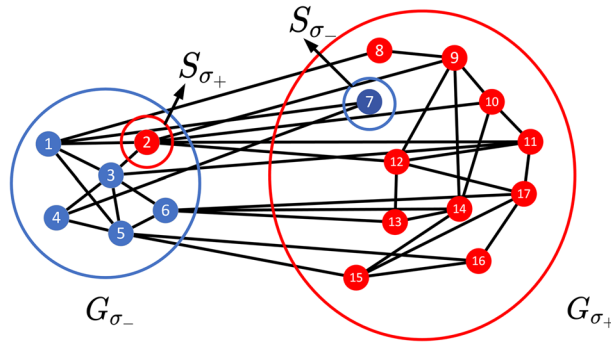


Fig. 4 State of a NCO system as in Fig. 3, but at time $t = t + 1$. Node 2 changes its opinion from σ_- to σ_+ , and node 7 changes its opinion from σ_+ to σ_- . Sets S_{σ_+} and S_{σ_-} consist of node 2 and node 7, respectively

$$f_{\sigma_+,fail} = \frac{\sum f''_{\sigma_-,d_{\sigma_-},d_{\sigma_+}} \cdot d_{\sigma_+}}{\sum f_{\sigma_+,d_{\sigma_-},d_{\sigma_+}} \cdot d_{\sigma_+}} \tag{6}$$

The fractions of links between the G_{σ_-} and G_{σ_+} subgraphs becoming links in the G_{σ_-} and G_{σ_+} subgraphs are respectively

$$f_{\sigma_-,add} = \frac{\sum f''_{\sigma_-,d_{\sigma_-},d_{\sigma_+}} \cdot d_{\sigma_-}}{\sum f_{\sigma_+,d_{\sigma_-},d_{\sigma_+}} \cdot d_{\sigma_-}} \tag{7}$$

and

$$f_{\sigma_+,add} = \frac{\sum f''_{\sigma_+,d_{\sigma_-},d_{\sigma_+}} \cdot d_{\sigma_+}}{\sum f_{\sigma_-,d_{\sigma_-},d_{\sigma_+}} \cdot d_{\sigma_+}} \tag{8}$$

Figure 5 shows an opinion changing process of G_{σ_-} subgraph. In Fig. 5a, there are $N_{\sigma_-} = 6$ nodes and $L = 9$ links in the G_{σ_-} subgraph. Node 2 has 6 links, two of them are connecting to σ_- nodes, the others are connecting to σ_+ nodes. In Fig. 5b, as node 2 changes its opinion, node 2 and link a, b are removed from the G_{σ_-} subgraph. Node 7 and link c, d join the G_{σ_-} subgraph. The fractions $f_{\sigma_-,fail}$ and $f_{\sigma_-,add}$ in this example are respectively $\frac{2}{9}$ and $\frac{2}{13}$.

Suppose there is a node l_- in $G_{\sigma_-} | S_{\sigma_+}$ and S_{σ_+} , and following one of its link l , node l_+ holding opinion σ_- is found, and l_- knows nothing about l_+ other than l_+ 's opinion. Since the nodes have no preference for neighbor, from l_- 's view, the probability that node l_+ 's opinion change equals to the fractions of link that are fail $f_{\sigma_-,fail}$. When l_+ 's opinion is σ_+ , the probability is $f_{\sigma_-,add}$. Then we know for a node with m σ_- neighbors and n σ_+ neighbors. Both for the σ_- and σ_+ nodes, their number of σ_- and σ_+ neighbors changes according to the binomial distribution. For nodes in $G_{\sigma_-} | S_{\sigma_+}$ and S_{σ_+} with m σ_- neighbors and n σ_+ neighbors, probabilities that e_- of its σ_- neighbors change their opinion and that e_+ of its σ_+ neighbors change their opinion are:

$$p_{\sigma_-,m}(e_-) = \binom{m}{e_-} \cdot f_{\sigma_-,fail}^{e_-} \cdot (1 - f_{\sigma_-,fail})^{m-e_-} \tag{9}$$

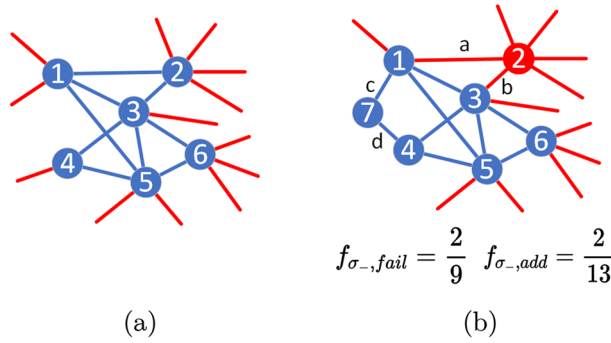


Fig. 5 Schematic representation of the neighbor opinion changing process of the G_{σ_-} subgraph. The colors of the links shows whether the link is connecting to a σ_- node (blue) or a σ_+ node (red). **a** State of the G_{σ_-} subgraph at time t . **b** State of the G_{σ_-} subgraph at time $t + 1$. Node 2 changes its opinion and be removed from G_{σ_-} subgraph. Node 7 changes its opinion and be added to G_{σ_-} subgraph

$$p_{\sigma_-,n}(e_+) = \binom{n}{e_+} \cdot f_{\sigma_-,add}^{e_+} \cdot (1 - f_{\sigma_-,add})^{n-e_+} \tag{10}$$

Similarly, for nodes in $G_{\sigma_+} | S_{\sigma_-}$ and S_{σ_-} , the probabilities are:

$$p_{\sigma_+,m}(e_-) = \binom{m}{e_-} \cdot f_{\sigma_+,add}^{e_-} \cdot (1 - f_{\sigma_+,add})^{m-e_-} \tag{11}$$

$$p_{\sigma_+,n}(e_+) = \binom{n}{e_+} \cdot f_{\sigma_+,fail}^{e_+} \cdot (1 - f_{\sigma_+,fail})^{n-e_+} \tag{12}$$

Given a node in $G_{\sigma_-} | S_{\sigma_+}$ and S_{σ_+} with m neighbors sharing its opinion and n σ_+ neighbors, the probability that this node evolves to have d_{σ_-} σ_- neighbors and d_{σ_+} σ_+ neighbors is:

$$p_{\sigma_-,m,n \rightarrow d_{\sigma_-}, d_{\sigma_+}} = \sum_{e_- \leq m, e_+ \leq n, m-e_-+e_+=d_{\sigma_-}} p_{\sigma_-,m}(e_-) \cdot p_{\sigma_-,n}(e_+) \tag{13}$$

Similarly, for a node in $G_{\sigma_+} | S_{\sigma_-}$ and S_{σ_-} with m σ_- neighbors and n neighbors sharing its opinion, the probability that it transitions to have d_{σ_-} σ_- neighbors and d_{σ_+} σ_+ neighbors is:

$$p_{\sigma_+,m,n \rightarrow d_{\sigma_-}, d_{\sigma_+}} = \sum_{e_- \leq m, e_+ \leq n, m-e_-+e_+=d_{\sigma_-}} p_{\sigma_+,m}(e_-) \cdot p_{\sigma_+,n}(e_+) \tag{14}$$

Figure 6 shows an example of computing the probability that a σ_- node with certain neighborhood opinion composition to another. In Fig. 6a, for a node in the σ_- subgraph the probability that its σ_+ neighbor change opinions is $\frac{1}{4}$. According to this probability, we can compute the probabilities that its two σ_+ neighbor keep their opinion, one keep its opinion and another change opinion, and both of this two neighbors change opinions. The probabilities are respectively $\frac{9}{16}$, $\frac{3}{8}$, and $\frac{1}{16}$. Based on the same computation, we can get the probabilities for its σ_- neighbors. In Fig. 6b, a σ_- node with 2 σ_- neighbors and 2 σ_+ neighbors can become a σ_- node with 3 σ_- neighbors and 1 σ_+ neighbor in two ways: 1.

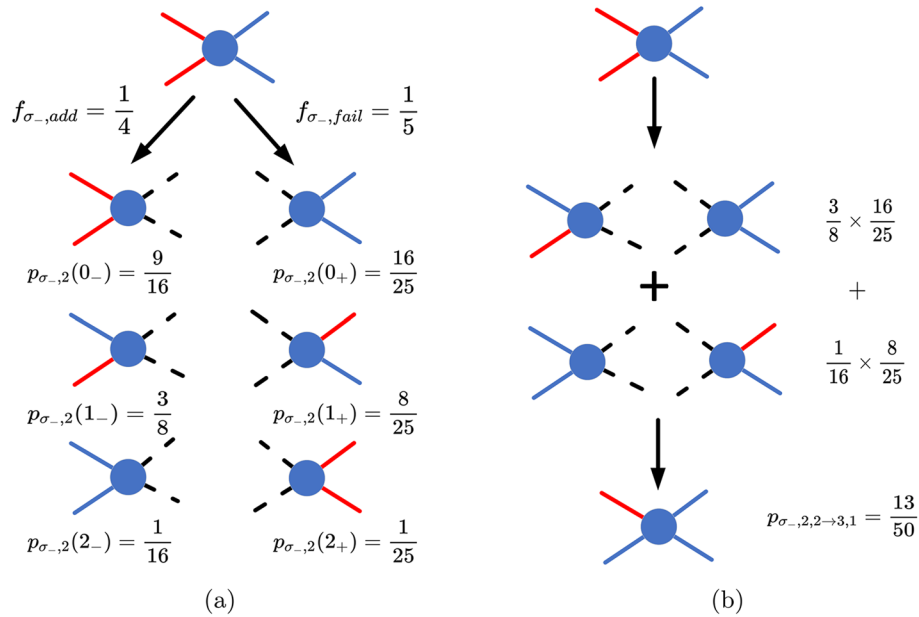


Fig. 6 An example of computing the probability that a σ_- node with 2 σ_- neighbors and 2 σ_+ neighbors changing to a σ_- node with 3 σ_- neighbors and 1 σ_+ neighbor. **a** Probabilistic neighbors state transition of a σ_- node with 2 σ_- neighbors and 2 σ_+ neighbors. **b** Probabilistic state transition of a σ_- node with 2 σ_- neighbors and 2 σ_+ neighbors

One of its σ_+ neighbor become σ_- neighbor, and the σ_- opinion neighbors keep their opinion. 2. Both of the σ_+ neighbors change their opinion, and one of its σ_- neighbor change its opinion. The probability that a σ_- node with 2 σ_- neighbors and 2 σ_+ neighbors become a σ_- node with 3 σ_- neighbors and 1 σ_+ neighbor equals to the probability that one of these two events happens, which is $p_{\sigma_-,2,2 \rightarrow 3,1} = \frac{3}{8} \times \frac{16}{25} + \frac{1}{16} \times \frac{8}{25} = \frac{13}{50}$.

Finally, the ratio of σ_- nodes and σ_+ that have m σ_- neighbors and n σ_+ neighbors after one iteration to the number of nodes that hold the σ_- opinion at the initial state are:

$$f_{\sigma_-,d_{\sigma_-},d_{\sigma_+}}(t+1) = \sum_{m+n=d_{\sigma_-}+d_{\sigma_+}} f'_{\sigma_-,m,n}(t) \cdot p_{\sigma_-,m,n \rightarrow d_{\sigma_-},d_{\sigma_+}} + \sum_{m+n=d_{\sigma_-}+d_{\sigma_+}} f''_{\sigma_-,m,n}(t) \cdot p_{\sigma_+,m,n \rightarrow d_{\sigma_-},d_{\sigma_+}} \quad (15)$$

$$f_{\sigma_+,d_{\sigma_-},d_{\sigma_+}}(t+1) = \sum_{m+n=d_{\sigma_-}+d_{\sigma_+}} f'_{\sigma_+,m,n}(t) \cdot p_{\sigma_+,m,n \rightarrow d_{\sigma_-},d_{\sigma_+}} + \sum_{m+n=d_{\sigma_-}+d_{\sigma_+}} f''_{\sigma_+,m,n}(t) \cdot p_{\sigma_-,m,n \rightarrow d_{\sigma_-},d_{\sigma_+}} \quad (16)$$

Figure 7 illustrates the entire flow of mean-field dynamics for the NCO model.

- (A) Given the fractions of nodes in different states of the system at a given time t , we calculate the fractions of nodes that change their opinions.
- (B) With the change of opinions of nodes in σ_- and σ_+ subgraphs, we get the fraction of links removed from (and added to) σ_- and σ_+ subgraphs.

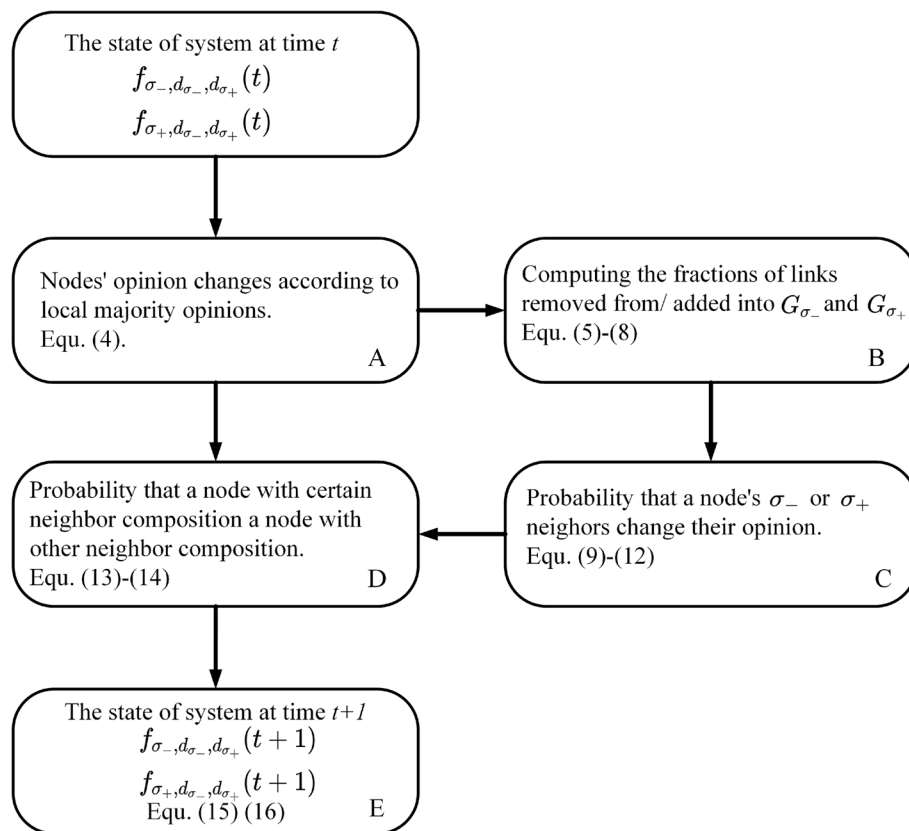


Fig. 7 Flowchart of mean-field dynamics for the NCO model

- (C) Based on the changes of links in the σ_- and σ_+ subgraphs, we get the probability that the neighbors of a node in σ_- and σ_+ subgraphs change their opinions.
- (D) According to the probability that a node's neighbor changes their opinion, we obtain the probability that nodes in certain state changes to other state.
- (E) Fractions of nodes in different states at time $t + 1$ are calculated according to the probability that the nodes in certain state change to other state.

We refer to the set of equations used to describe the dynamics of the NCO model in this section as the Mean-Field NCO governing equation.

Simulation results and discussions

The time complexity of the Monte-Carlo simulation of NCO model is $O(MD_{\max}N)$, where M is the number of repetitions of the simulation, D_{\max} is the maximum degree in the network and N is the number of nodes in the network. Estimating the opinion fraction through simulation is clearly very time-consuming. The mean-field dynamics of the NCO model provide a faster way to estimate the opinion fraction F at time t for a specific random graph. The time complexity of this method is $O(D_{\max}^2)$. For the Monte Carlo simulation method, to achieve high simulation accuracy, we need to perform the simulation many times. However, for the mean-field method, only a single numerical integration is required. Theoretically, the maximum degree in a network can be $N - 1$, but the probability of nodes with

extremely large degrees is very low. Considering this low probability, we disregard these nodes in practical calculations. We set a degree truncation threshold (DTT) D_{\max} according to the following truncation criterion inequality:

$$\frac{\sum_{k=0}^{D_{\max}} \theta_k \cdot k}{\sum_{k=0}^{N-1} \theta_k \cdot k} > 1 - \eta \tag{17}$$

$$D_{\max} = \min_{d \in \mathbb{Z}} \left\{ d \mid \frac{\sum_{k=0}^d \theta_k \cdot k}{\sum_{k=0}^{N-1} \theta_k \cdot k} > 1 - \eta \right\} \tag{18}$$

where θ_k represents the fraction of nodes with degree k . The accuracy of the prediction results increases as η decreases. For Erdős–Rényi (ER) graphs, the degree truncation threshold (DTT) D_{\max} equals:

$$D_{\max} = \left\lceil \mu + \sigma \Phi^{-1} \left(\sigma(1 - \eta) + \frac{\sigma}{\mu\sqrt{2\pi}} \exp\left(-\frac{\mu^2}{2\sigma^2}\right) + \Phi\left(-\frac{\mu}{\sigma}\right) \right) \right\rceil \tag{19}$$

where $\mu = (N - 1)p$, $\sigma = \sqrt{Np(1 - p)}$, and Φ is the cumulative distribution function of the standard normal distribution. For Barabási-Albert (BA) models, the degree truncation threshold (DTT) D_{\max} equals:

$$D_{\max} = \left\lceil \frac{N - m - 1 + 2N - 2m - 2\eta N + 2\eta m}{1 + \eta N + m - \eta m} \right\rceil \tag{20}$$

The derivation of these two DTTs is given in Appendix . In this paper, we set $\eta = 10^{-5}$ for ER graphs, and $\eta = 10^{-3}$ for BA models. We set a larger η for BA models because BA models have more heterogeneous degree distributions.

Opinion fraction F

We first investigate the NCO governing equations described in “[Mean-field dynamics of NCO model](#)” section on Erdős–Rényi (ER), Barabási-Albert (BA) and configuration models by comparing the Monte–Carlo simulation results and the estimation results of the opinion fraction F at time t .

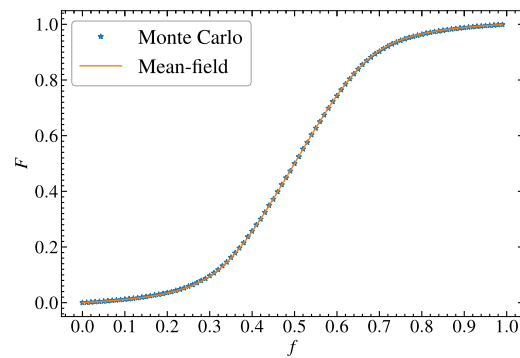
The σ_- opinion fraction at time t is denoted as:

$$F(t) = \sum_{d_{\sigma_-} + d_{\sigma_+} = 0}^{D_{\max}} f_{\sigma_-, d_{\sigma_-}, d_{\sigma_+}}(t) \tag{21}$$

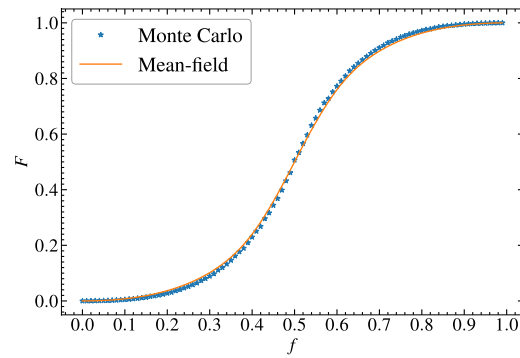
Theoretically, there is always a possibility that the system will continue to iterate. We set the iteration to stop when the rate of change of the final opinion fraction is less than a tiny value ϵ , denoted as:

$$|F(t + 1) - F(t)| < \epsilon \tag{22}$$

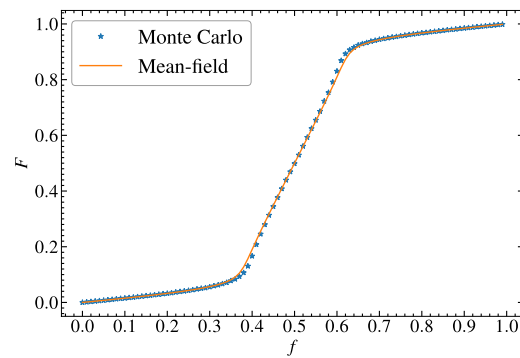
In this paper, we set $\epsilon = 10^{-5}$. Figure 8 presents the simulation and estimation results of Erdős–Rényi graphs ($N = 10,000$, $p = 0.0004$), Barabási-Albert graphs ($N = 10,000$, $k_{\min} = 2$), and configuration models (with degree distribution



(a) ER networks with $N = 10000$, $p = 0.0004$.



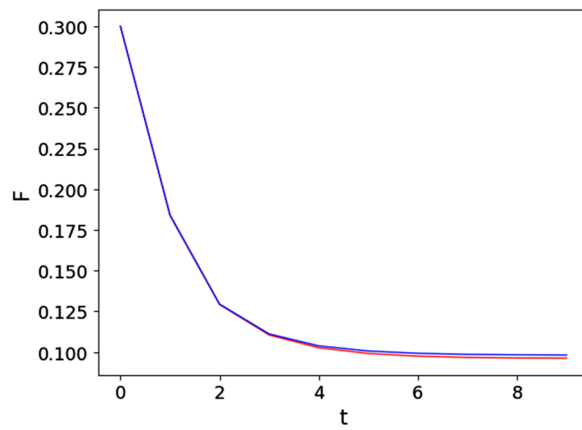
(b) Barabási–Albert (BA) model with $N = 10000$, number of edges added per step $m = 2$.



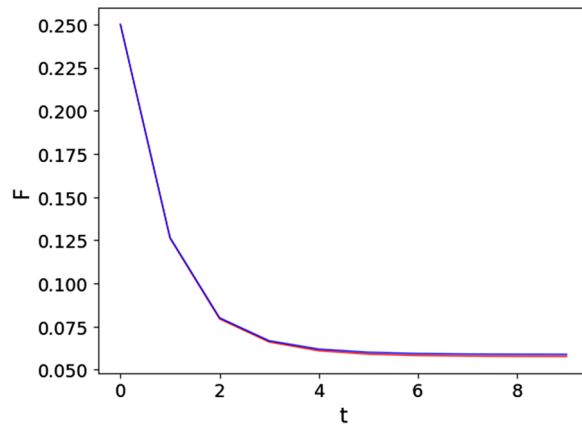
(c) Configuration model with $N = 10000$ and a random degree distribution.

Fig. 8 Simulation results and mean-field estimations of the final opinion fraction F as a function of initial opinion fraction f for different network models

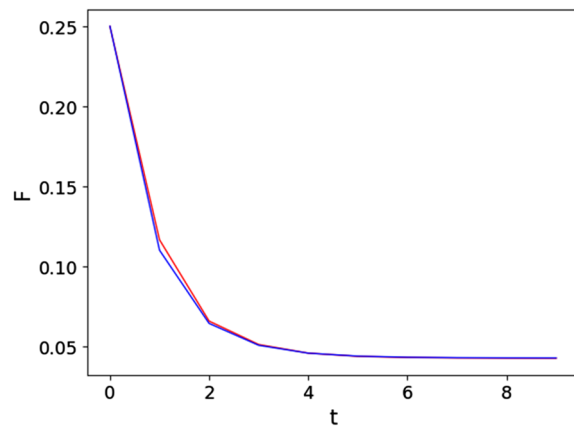
$D = [0.0, 0.147, 0.106, 0.045, 0.153, 0.158, 0.089, 0.124, 0.039, 0.138]$). Averages over 1000 realizations are shown for all curves. Figure 9 illustrates the simulation and estimation results for the degree distribution of the σ_- nodes at time t . As shown in the figures, the NCO governing equations provide a good estimate of the opinion fraction in the non-consensus model.



(a) ER networks with $N = 10000$, $p = 0.0004$.



(b) Barabási–Albert (BA) model with $N = 10000$, number of edges added per step $m = 2$.



(c) Configuration model with $N = 10000$ and a random degree distribution.

Fig. 9 The simulation result and mean-field estimation of the opinion fraction $F(t)$ as a function of time t

Although the estimated results of final opinion fraction F are very close to the simulation results, there are still some differences between them. Two factors may contribute to this discrepancy:

- Some nodes with very large degrees are ignored when performing the estimation, which can be improved by reducing the value of η .
- The size of the network used for simulation may not be sufficiently large. Limited by computer resources, the maximum network size used in our experiments is only 10,000, which may not be sufficiently large to approximate the asymptotic result of the NCO mean-field model.

Critical threshold of NCO model

The critical threshold of the NCO model is defined as a specific initial opinion fraction, denoted as f_c . Below this threshold, only scattered clusters exist in the steady state. However, once the initial opinion fraction surpasses f_c , the system can exhibit a giant component. The emergence of giant components implies that nodes holding a minority opinion in the steady state form non-invasive clusters, whose size is proportional to the size of the network, allowing the minority opinion to stably exist in the steady state. The critical threshold is marked by the peak in the relative size of the second largest cluster. The NCO governing equations described in “[Mean-field dynamics of NCO model](#)” section offer a method for determining this critical threshold. Through iterative computations, we obtain the fractions of σ_- nodes with different neighbor compositions in the steady state. Based on these fractions we can get the degree distribution of nodes within the σ_- subgraph by

$$P_{D=d_{\sigma_-}} = \sum_{j=0}^{D_{\max}-d_{\sigma_-}} f_{\sigma_-,d_{\sigma_-},j} \tag{23}$$

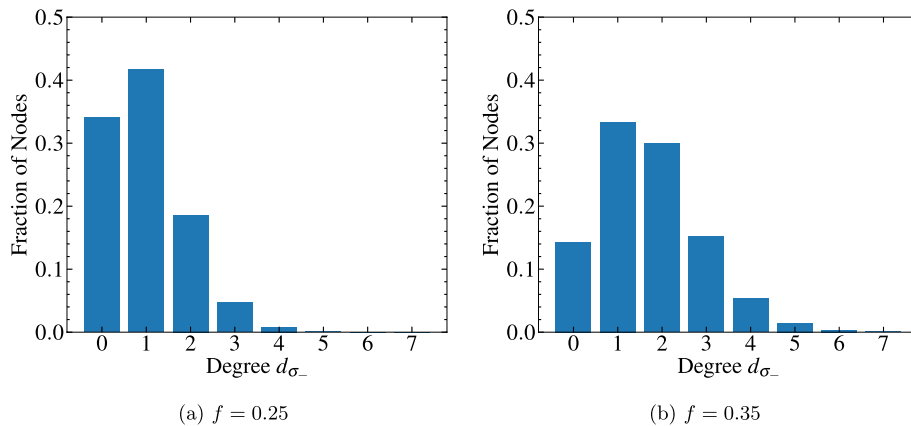


Fig. 10 The degree distributions of the σ_- subgraph at two steady states with different initial opinion fraction f of a NCO system in ER networks with $N = 10,000, p = 0.0004$

Additionally, by calculating the first and second-order moments of the degree distribution, we can identify the presence of giant components. For random graphs where giant components exist, the following criteria apply (Van Mieghem et al. 2014):

$$E[k^2] - 2 \cdot E[k] > 0 \tag{24}$$

Figure 10 presents the degree distributions of the σ_- subgraph at two steady states of an NCO system in an ER network with $N = 10,000$ and $p = 0.0004$. Figure 10a shows the degree distribution of the σ_- subgraph at steady state for an initial opinion fraction of $f = 0.25$, and Fig. 10b for $f = 0.35$. The values of $E[k^2] - 2 \cdot E[k]$ for the two cases are respectively -0.1898 and 0.8768 . For an initial opinion fraction of $f = 0.25$, there is no giant component of the σ_- opinion in the steady state, while for $f = 0.35$, a giant component will form.

Figure 11 presents the values of $E[k^2] - 2 \cdot E[k]$ and the second largest cluster as functions of the initial opinion fraction f for ER, BA model, and configuration model networks. The red star marks the zero-crossing point of the $E[k^2] - 2 \cdot E[k]$ curve, which shows the critical threshold f_c derived through NCO governing equation. According to Fig. 11, the critical thresholds f_c , obtained through the NCO governing equation are very close to the critical thresholds derived through simulations.

Size of the largest cluster

The size of the largest σ cluster can also be obtained using the NCO governing equation. Newman et al. (2001), Van Mieghem et al. (2014) proposed a method to estimate the size of the giant component in random graphs with arbitrary degree distributions, employing the probability generating function (pgf). The degree distribution of the σ_- subgraph at the steady state is obtained in the same manner as described in “Critical threshold of NCO model” section. Given this degree distribution, we define the degree generating function as follows:

$$\varphi_D(z) = \mathbb{E}[z^D] = \sum_{j=0}^{N-1} \Pr[D = j] \cdot z^j \tag{25}$$

Here, $\varphi_D(z)$ denotes the degree generating function, where $\mathbb{E}[z^D]$ represents the expected value of z raised to the power of degree D , and $\Pr[D = j]$ is the probability of a node having degree j .

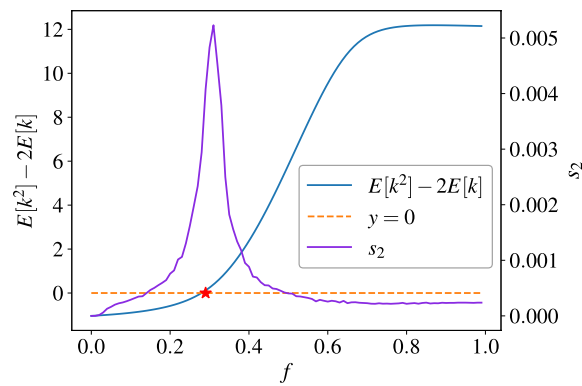
For an arbitrarily chosen link l and its endpoint l^+ , the pgf of the degree D_{l^+} minus 1 is:

$$\varphi_{D_{l^+}-1}(z) = \mathbb{E}[z^{D_{l^+}-1}] = \frac{\varphi'_D(z)}{\varphi'_D(1)} \tag{26}$$

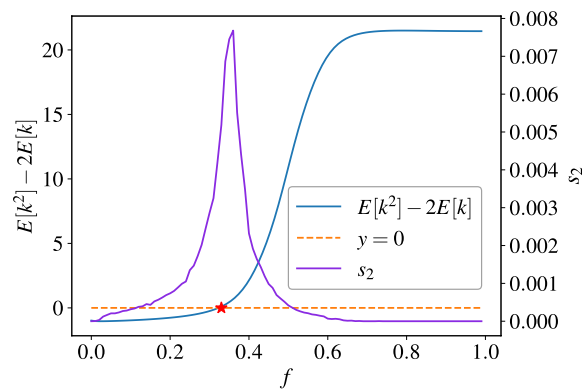
This equation, $\varphi_{D_{l^+}-1}(z)$, represents the pgf for the degree at endpoint l^+ , decreased by 1. Here, $\varphi'_D(z)$ is the first derivative of $\varphi_D(z)$, and $\varphi'_D(1)$ is its value at $z = 1$.

Finally, the normalized size of the largest cluster, s_1 , can be derived using:

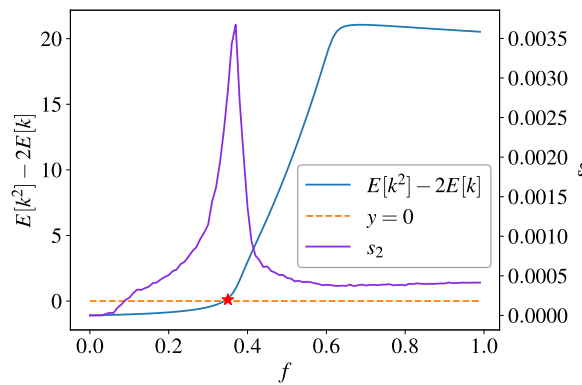
$$u = \varphi_{D_{l^+}-1}(u), \quad s_1 = 1 - \varphi_D(u) \tag{27}$$



(a) ER networks with $N = 10000$, $p = 0.0004$



(b) Barabási–Albert (BA) model with $N = 10000$, number of edges added per step $m = 2$.

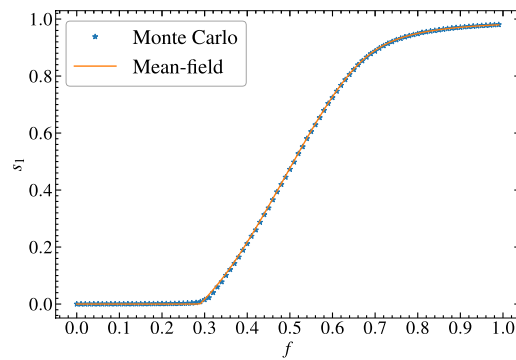


(c) Configuration model with $N = 10000$ and a random degree distribution.

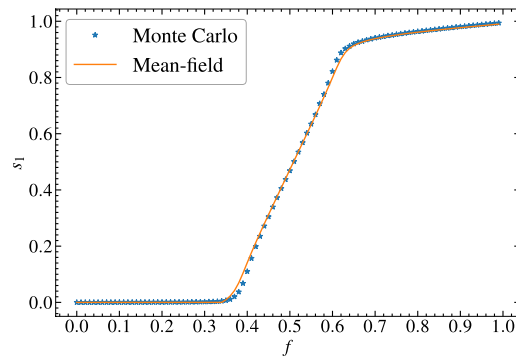
Fig. 11 Simulation results of the normalized second largest cluster s_2 and the value of $E[k^2] - 2 \cdot E[k]$ obtained from mean-field estimations. $\epsilon = 1 \times 10^{-5}$. The intersection of the $E[k^2] - 2 \cdot E[k]$ curve with the $y = 0$ curve is the estimate of the critical threshold f_c

In this formulation, u is the solution to the equation involving the pgf, and once found, it allows for calculating the normalized size of the largest component s_1 .

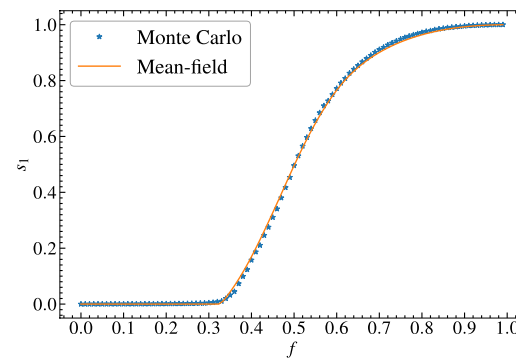
Figure 12 shows the relative size of the largest connected cluster at steady state, as obtained by simulation and the NCO governing equation. From these figures, we find



(a) ER networks with $N = 10000$, $p = 0.0004$.



(b) Barabási–Albert (BA) model with number of nodes $N = 100$, number of edges added per step $m = 2$.



(c) Configuration model with a random degree distribution.

Fig. 12 The simulation result and estimation of the relative size of the largest σ_- cluster s_1

that the size of the largest cluster can be accurately derived through the NCO governing equation.

Scale invariance of the NCO model

In the mean-field NCO model, the state of the system is represented by the fractions of nodes in different states in the system as $s = \{f_{\sigma,0,0}, \dots, f_{\sigma,i,j}, \dots\}$. For NCO systems with different numbers of nodes, if the initial states $s(0)$ are the same, the subsequent

states $s(t)$ will also be the same. The fractions of nodes in different states in the initial state depend on the degree distribution of the network. For networks with different numbers of nodes, as long as their degree distributions are the same, the initial state $s(0)$ will be the same, and thus the subsequent states will also be the same.

The degree distribution of an ER graph follows a binomial distribution $B(N, p)$. The binomial distribution $B(N, p)$ can be approximated by a Poisson distribution $\text{Poisson}(\lambda)$ when N is large and p is small, such that the mean $\lambda = Np$ remains sufficiently small (Ross 2014).

Under these conditions, the binomial distribution $B(N, p)$ can be approximated by a Poisson distribution with $\lambda = Np$:

$$B(N, p) \sim \text{Poisson}(\lambda)$$

Thus, when N is large, the degree distribution of an ER graph approximately equals the probability mass function (PMF) of a Poisson distribution:

$$P[D = k] = \frac{\lambda^k e^{-\lambda}}{k!} \tag{28}$$

If the average degree $\bar{k} = Np$ of two ER networks is the same, the degree distributions of these two networks are approximately equal, which is $\text{Poisson}(\bar{k})$. Figure 13 shows the Monte Carlo simulation results of the final opinion fraction F as a function of the initial opinion fraction f for two ER graphs with different numbers of nodes N and the same average degree \bar{k} . As we expect, the final opinion fractions of two ER graphs with different numbers of nodes N but the same average degree \bar{k} are highly similar.

Degree variation in the NCO model

Nodes with different degrees have different behaviors in the NCO model. To study the behavior of nodes with varying degrees, we conduct simulations on the configuration model graph with a uniform degree distribution, where the fractions of nodes at each degree are the same. This graph was chosen as the experimental network due to the ease

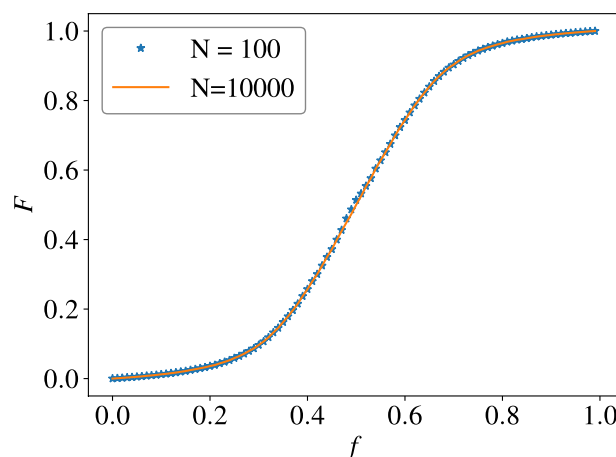


Fig. 13 Monte–Carlo simulation of the final opinion fraction F as a function of initial opinion fraction f for two ER graphs with $N = 100, p = 0.04$ and $N = 10,000, p = 0.0004$

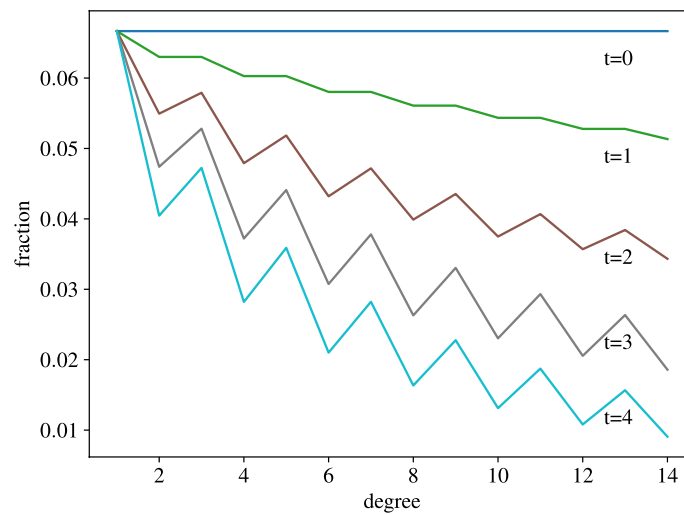


Fig. 14 The fraction of σ_- nodes as a function of node degree in the configuration model network based on a uniform degree distribution ($N = 10,000, d_{\min} = 1, d_{\max} = 16$) for different time slot t . The initial opinion fraction $f = 0.45$

of observation. Figure 14 shows how the fractions of σ_- nodes with different degrees change over time. From Fig. 14, we find that

- Among the σ_- opinion nodes, nodes with higher degree are more likely to change their opinions to σ_+ .
- Odd-degree nodes ($d = 2n + 1$) are more resistant to opinion change compared to even-degree nodes ($d = 2n$).

For nodes with high degrees, their individual opinions count less weight within their local opinions, making them more responsive to the prevailing global consensus. Consequently, nodes with high degrees are more likely to change their opinions.

According to the analysis in “Mean-field dynamics of NCO model” section, the probability of the number of σ_- neighbors of a node becoming σ_+ neighbors follows the binomial distribution. Normally, those minority opinion σ_- nodes with higher degree has more σ_- neighbors than those with lower degree. This means σ_- nodes with high degree are more likely to lose σ_- neighbors, and more likely to become a node with more σ_+ neighbors than σ_- neighbors. Thus nodes with higher degree are more likely to change their opinions.

Another intriguing phenomenon we have noticed is that odd-degree nodes ($d = 2n + 1$) are more resistant to opinion change compared to even-degree nodes ($d = 2n$). Surprisingly, despite odd-degree nodes having one more neighbor compared to even-degree nodes with one less neighbor, the probability of odd-degree nodes being influenced is lower than that of even-degree nodes.

The probability of opinion change for even-degree σ_- nodes with $d = 2n$ and $\mathcal{N}_{\sigma_-,v} = i$, and odd-degree σ_- nodes with $d = 2n + 1$ and $\mathcal{N}_{\sigma_-,v} = i$ can be expressed as follows:

$$p_{\text{even},i,2n+1-i} = \sum_{e_- < i} \sum_{i - e_- + e_+ < n} p_{\sigma_-,i}(e_-) \cdot p_{\sigma_+,2n+1-i}(e_+), \tag{29}$$

$$p_{\text{odd},i,2n-i} = \sum_{e_- < i} \sum_{i - e_- + e_+ < n} p_{\sigma_-,i}(e_-) \cdot p_{\sigma_+,2n-i}(e_+). \tag{30}$$

Now, we analyze the difference between $p_{\text{odd},i}$ and $p_{\text{even},i}$:

$$\begin{aligned} & p_{\text{odd},i,2n+1-i} - p_{\text{even},i,2n-i} \\ &= \sum_{e_- < i} p_{\sigma_-,i}(e_-) \cdot (\Pr[X_1 < n - i + e_-] - \Pr[X_2 < n - i + e_-]) < 0 \end{aligned} \tag{31}$$

where X_1, X_2 follows binomial distributions $B(2n + 1 - i, p_{\sigma_-,add}), B(2n - i, p_{\sigma_-,add})$.

For the two binomial distribution with same p and same required successes number, the larger the number of Bernoulli trials, the higher the probability, and thus $\Pr[X_1 < n - i + e_-] - \Pr[X_2 < n - i + e_-] < 0$. Therefore, we can conclude that, for nodes with the same number of σ_- neighbors, even-degree nodes are more likely to change their opinions compared to odd-degree nodes. This explains to some extent why the opinions of nodes of odd degree are more stable.

Behavioural trends in NCO models

The behavioral logic of nodes in the NCO model is to adopt the local majority opinion. From each node’s perspective, this results in a decrease in the number of neighboring nodes that hold a different opinion. Generally, from a global perspective, the consequence of each node adopting this behavior is a decrease in the number of links connecting nodes with dissenting opinions after each opinion change. This trend is realized in two ways:

- The decrease in the number of nodes holding the minority opinion. Like the example in Fig. 15 shows, the number of minority opinion (red) nodes decrease from 4 to 1. The number of links connecting red and blue opinion nodes decreases from 12 to 1.
- The formation of separated σ_- and σ_+ clusters in the network, where nodes in each cluster have more connections to each other than to other clusters. As illustrated in

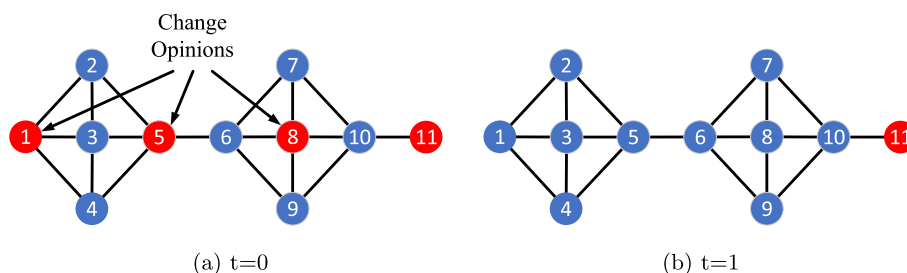


Fig. 15 Dynamics of the NCO model on a network with $N = 11$ nodes. **a** At $t = 0$, 4 nodes are assigned with a red opinion, and the other 7 nodes with a blue opinion. The local majority opinion for node 1, 5, 8 are blue, and they will change their opinions. **b** At $t = 1$, all nodes in the system are holding a local majority opinion. The system has reached a steady state

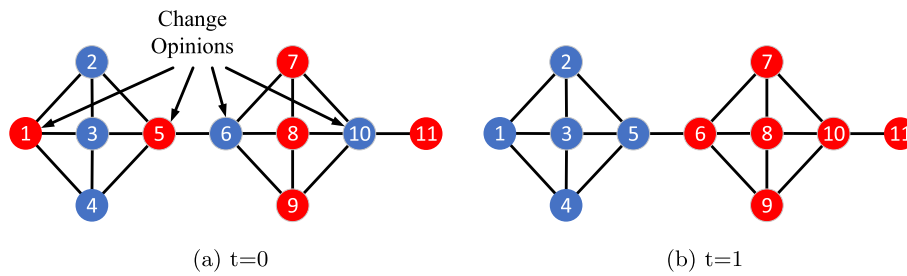


Fig. 16 Dynamics of the NCO model on a network with $N = 11$ nodes. **a** At $t = 0$, 6 nodes are assigned with a red opinion, and the other 5 nodes with a blue opinion. The local majority opinion for node 1, 5, 6, 10 are different with their own current opinion, and they will change their opinions. **b** At $t = 1$, all nodes in the system are holding a local majority opinion. The system has reached a steady state

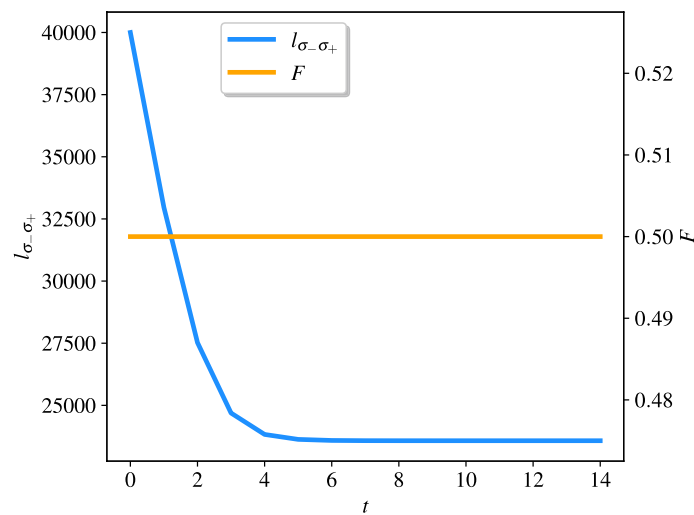


Fig. 17 Number of links between σ_- and σ_+ subgraphs $l_{\sigma_- \sigma_+}$ and the opinion fraction $F(t)$ as functions of time t of the dynamics of the NCO model in the Configuration Model network with a uniform degree distribution ($N = 10,000, d_{\min} = 1, d_{\max} = 16$) and $f = 0.5$

Fig. 16, nodes 1–5 form a blue opinion cluster, while nodes 6–11 form a red opinion cluster. The number of links connecting red and blue opinion nodes decreases from 14 to 1.

To study the behavioral trends in the NCO model for large-sized graphs, we perform simulations on a configuration model network with a uniform degree distribution ($N = 10,000, d_{\min} = 1,$ and $d_{\max} = 16$) with initial opinion fractions $f = 0.45$ and $f = 0.5$. When the fractions of σ_- and σ_+ are the same at the initial state, as shown in Fig. 17, the fraction of σ_- nodes $F(t)$ does not change over time. However, the number of links between σ_- and σ_+ subgraphs $l_{\sigma_- \sigma_+}$ decreases as time progresses. Figure 18 shows that after each iteration both the the fraction of σ_- nodes $F(t)$ and the number of links between σ_- and σ_+ subgraphs $l_{\sigma_- \sigma_+}$ decrease. Additionally, in first several time slots, $l_{\sigma_- \sigma_+}$ doesn't decrease proportionally with $F(t)$, which means minority opinion nodes with more majority opinion neighbors are more likely to change their opinions. These

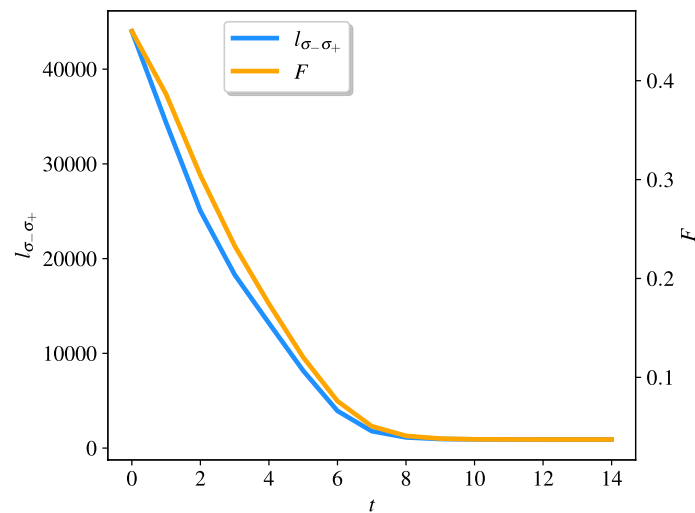


Fig. 18 Number of links between σ_- and σ_+ subgraphs $l_{\sigma_- \sigma_+}$ and the opinion fraction $F(t)$ as functions of time t of the dynamics of the NCO model in the Configuration Model network with a uniform degree distribution ($N = 10,000$, $d_{\min} = 1$, $d_{\max} = 16$) and $f = 0.45$

figures also illustrate how the number of links between the σ_- and σ_+ subgraphs changes over time for these two cases.

Conclusion

To enhance further understanding of the Non-Consensus Opinion (NCO) model, we derived in this paper a mean-field-based description for the NCO model under the assumption of low degree–degree correlation. The mean-field NCO equations merely require knowledge on a node’s own current opinion and the number of its σ_- and σ_+ neighbors but does not require any knowledge on the exact network structure. The basic assumption of the mean-field dynamics in the configuration model of the NCO model is that, at each iteration, the σ_- (σ_+) neighboring nodes of a node change its opinion according to a certain probability. This probability can be obtained from the fractions of nodes in different states. Important parameters such as the fraction of a certain opinion F , the critical threshold f_c , and the size of the largest connected cluster for a given opinion s_1 can be derived using this mean-field method. Simulation results show that this mean-field dynamics can effectively approximate F , f_c , and s_1 . This mean-field description provides an analytical way to explain some phenomena observed in the NCO model. The scale invariance of the NCO model is discussed. The variation in the degrees of nodes with different opinions in the dynamics of the NCO model is also investigated. We explain why nodes with minority opinions and greater degrees are more likely to change their opinions in the NCO model. We also explain why nodes with minority opinions and even degrees are more likely to change their opinions than those with odd degrees. Additionally, we reveal that, in most cases, the dynamics of the NCO model tends toward a decrease in the number of links connecting nodes with different opinions.

The mean-field description given in this study can be used in studies of other spin-type opinion models. In particular, the mean-field equations are beneficial in spin-type opinion models where exact solutions are scarce and simulations time-consuming. Analysing phase

transitions and other key properties of the opinion models are much easier and insightful with the help of our mean-field method. An open question is whether a similar method can be derived for networks with a large degree-degree correlation.

Appendix 1: Degree truncation threshold (DTT)

Appendix 1.1: Erdős-Rényi (ER) Graph

For an Erdős-Rényi (ER) graph, the degree distribution θ_k follows a binomial distribution:

$$\theta_k = \binom{N-1}{k} p^k (1-p)^{N-1-k} \tag{32}$$

Then we obtain that:

$$\begin{aligned} & \frac{\sum_{k=0}^{D_{\max}} \theta_k \cdot k}{\sum_{k=0}^{N-1} \theta_k \cdot k} \\ &= \frac{\sum_{k=0}^{D_{\max}} k \binom{N-1}{k} p^k (1-p)^{N-1-k}}{\sum_{k=0}^{N-1} k \binom{N-1}{k} p^k (1-p)^{N-1-k}} \end{aligned} \tag{33}$$

The term $\binom{N-1}{k} p^k (1-p)^{N-1-k}$ is the probability density function (PDF) of the binomial distribution. According to the Central Limit theorem (Van Mieghem et al. 2014; Walker and Helen 1985), the binomial distribution approximately equals the normal distribution for large N . The truncation criterion function of ER graph can then be approximated as follows:

$$\begin{aligned} & \frac{\sum_{k=0}^{D_{\max}} k \binom{N-1}{k} p^k (1-p)^{N-1-k}}{\sum_{k=0}^{N-1} k \binom{N-1}{k} p^k (1-p)^{N-1-k}} \\ &= \frac{\sum_{k=0}^{D_{\max}} k \binom{N-1}{k} p^k (1-p)^{N-1-k}}{\mu} \\ &= \frac{\int_0^{D_{\max}} k \frac{1}{\sqrt{2\pi}\sigma} \exp\left(-\frac{(\mu-k)^2}{2\sigma^2}\right) dk}{\mu} \end{aligned} \tag{34}$$

where $\mu = (N-1)p$ and $\sigma = \sqrt{(N-1)p(1-p)}$.

To get D_{\max} , we need to solve the following truncation criterion inequality:

$$\frac{\int_0^{D_{\max}} k \frac{1}{\sqrt{2\pi}\sigma} \exp\left(-\frac{(\mu-k)^2}{2\sigma^2}\right) dk}{\mu} > 1 - \eta \tag{35}$$

Next, rearrange to solve for the integral:

$$\int_0^{D_{\max}} k \frac{1}{\sqrt{2\pi}\sigma} \exp\left(-\frac{(\mu-k)^2}{2\sigma^2}\right) dk > (1 - \eta)\mu \tag{36}$$

Let Z be the standard normal variable:

$$Z = \frac{k - \mu}{\sigma}$$

Then,

$$dk = \sigma dZ \quad \text{and} \quad k = \mu + \sigma Z$$

Substitute k and dk into the integral:

$$\int_{-\frac{\mu}{\sigma}}^{\frac{D_{\max} - \mu}{\sigma}} (\mu + \sigma Z) \frac{1}{\sqrt{2\pi}\sigma} \exp\left(-\frac{Z^2}{2}\right) \sigma dZ > (1 - \eta)\mu \tag{37}$$

This simplifies to:

$$\int_{-\frac{\mu}{\sigma}}^{\frac{D_{\max} - \mu}{\sigma}} \left(\frac{\mu}{\sigma} \frac{1}{\sqrt{2\pi}} \exp\left(-\frac{Z^2}{2}\right) + \frac{\sigma Z}{\sqrt{2\pi}} \exp\left(-\frac{Z^2}{2}\right) \right) dZ > (1 - \eta)\mu \tag{38}$$

Recognize the integrals:

$$\frac{\mu}{\sigma} \int_{-\frac{\mu}{\sigma}}^{\frac{D_{\max} - \mu}{\sigma}} \frac{1}{\sqrt{2\pi}} \exp\left(-\frac{Z^2}{2}\right) dZ + \sigma \int_{-\frac{\mu}{\sigma}}^{\frac{D_{\max} - \mu}{\sigma}} \frac{Z}{\sqrt{2\pi}} \exp\left(-\frac{Z^2}{2}\right) dZ > (1 - \eta)\mu \tag{39}$$

The first integral:

$$\frac{\mu}{\sigma} \int_{-\frac{\mu}{\sigma}}^{\frac{D_{\max} - \mu}{\sigma}} \frac{1}{\sqrt{2\pi}} \exp\left(-\frac{Z^2}{2}\right) dZ = \frac{\mu}{\sigma} \left(\Phi\left(\frac{D_{\max} - \mu}{\sigma}\right) - \Phi\left(-\frac{\mu}{\sigma}\right) \right) \tag{40}$$

where Φ is the cumulative distribution function of the standard normal distribution.

The second integral:

$$\begin{aligned} & \sigma \int_{-\frac{\mu}{\sigma}}^{\frac{D_{\max} - \mu}{\sigma}} \frac{Z}{\sqrt{2\pi}} \exp\left(-\frac{Z^2}{2}\right) dZ \\ &= -\frac{\sigma}{\sqrt{2\pi}} \exp\left(-\frac{Z^2}{2}\right) \Big|_{Z=-\frac{\mu}{\sigma}}^{\frac{D_{\max} - \mu}{\sigma}} \\ &= \frac{\sigma}{\sqrt{2\pi}} \left(\exp\left(-\frac{(D_{\max} - \mu)^2}{2\sigma^2}\right) - \exp\left(-\frac{\mu^2}{2\sigma^2}\right) \right) \end{aligned}$$

In general D_{\max} is large, thus $\exp\left(-\frac{(D_{\max} - \mu)^2}{2\sigma^2}\right) \approx 0$. Then we obtain:

$$\sigma \int_{-\frac{\mu}{\sigma}}^{\frac{D_{\max} - \mu}{\sigma}} \frac{Z}{\sqrt{2\pi}} \exp\left(-\frac{Z^2}{2}\right) dZ \approx -\frac{\sigma}{\sqrt{2\pi}} \exp\left(-\frac{\mu^2}{2\sigma^2}\right)$$

Finally, the truncation criterion inequality becomes:

$$\frac{\mu}{\sigma} \left(\Phi\left(\frac{D_{\max} - \mu}{\sigma}\right) - \Phi\left(-\frac{\mu}{\sigma}\right) \right) - \frac{\sigma}{\sqrt{2\pi}} \exp\left(-\frac{\mu^2}{2\sigma^2}\right) > (1 - \eta)\mu \tag{41}$$

Solve for D_{\max} :

$$D_{\max} = \left\lceil \mu + \sigma \Phi^{-1} \left(\sigma(1 - \eta) + \frac{\sigma}{\mu\sqrt{2\pi}} \exp\left(-\frac{\mu^2}{2\sigma^2}\right) + \Phi\left(-\frac{\mu}{\sigma}\right) \right) \right\rceil \tag{42}$$

Appendix 1.2: Barabási-Albert (BA) model

For an Barabási-Albert (BA) model, the degree distribution θ_k follows a binomial distribution (Pósfai and Barabási 2016):

$$\theta_k = \frac{2m(m + 1)}{k(k + 1)(k + 2)} \tag{43}$$

Then we obtain that:

$$\begin{aligned} & \frac{\sum_{k=0}^{D_{\max}} \theta_k \cdot k}{\sum_{k=0}^{N-1} \theta_k \cdot k} \\ &= \frac{\sum_{k=m}^{D_{\max}} \frac{2m(m+1)}{(k+1)(k+2)}}{\sum_{k=m}^{N-1} \frac{2m(m+1)}{(k+1)(k+2)}} \\ &= \frac{\frac{1}{m+1} - \frac{1}{D_{\max}+2}}{\frac{1}{m+1} - \frac{1}{N+1}} \\ &= \frac{(D_{\max} + 1 - m)(N + 1)}{(D_{\max} + 2)(N - m)} \end{aligned} \tag{44}$$

Then we obtain the truncation criterion inequality:

$$\frac{(D_{\max} + 1 - m)(N + 1)}{(D_{\max} + 2)(N - m)} > 1 - \eta \tag{45}$$

Finally, solve for D_{\max} :

$$D_{\max} = \left\lceil \frac{N - m - 1 + 2N - 2m - 2\eta N + 2\eta m}{1 + \eta N + m - \eta m} \right\rceil \tag{46}$$

Author contributions

Xinhan Liu proposed this mean-field based theory, and did all the simulations. A wrote the main manuscript text. All authors reviewed the manuscript.

Data availability

No datasets were generated or analysed during the current study.

Declarations

Competing interests

The authors declare no competing interests.

Received: 30 April 2024 Accepted: 2 August 2024

Published online: 20 August 2024

References

- Aletti G, Naimzada AK, Naldi G (2010) Mathematics and physics applications in sociodynamics simulation: the case of opinion formation and diffusion. In: *Mathematical modeling of collective behavior in socio-economic and life sciences*. Springer, pp 203–221
- Ben-Avraham Daniel (2011) Exact solution of the nonconsensus opinion model on the line. *Phys Rev E Stat Nonlinear Soft Matter Phys* 83(5):050101
- French JR Jr (1956) A formal theory of social power. *Psychol Rev* 63(3):181
- Galam S (2002) Minority opinion spreading in random geometry. *Eur Phys J B Condens Matter Complex Syst* 25:403–406
- Galam Serge (2008) Sociophysics: a review of Galam models. *Int J Mod Phys C* 19(03):409–440
- Galam S, Gefen Y, Shapir Y (1982) Sociophysics: a new approach of sociological collective behaviour. I. Mean-behaviour description of a strike. *J Math Sociol* 9(1):1–13
- Hassani H, Razavi-Far R, Saif M, Chiclana F, Krejcar O, Herrera-Viedma E (2022) Classical dynamic consensus and opinion dynamics models: a survey of recent trends and methodologies. *Inf Fus* 88:22–40
- Lambiotte R, Redner S (2008) Dynamics of non-conservative voters. *Europhys Lett* 82(1):18007
- Li Q, Braunstein LA, Havlin S, Stanley HE (2011) Strategy of competition between two groups based on an inflexible contrarian opinion model. *Phys Rev E* 84(6):066101
- Li Q, Braunstein LA, Wang H, Shao J, Stanley HE, Havlin S (2013) Non-consensus opinion models on complex networks. *J Stat Phys* 151:92–112
- Liu X, Achterberg MA, Kooij RE (2023) Non-consensus opinion models with malicious nodes. Available at SSRN 4421897
- Newman MEJ, Strogatz SH, Watts DJ (2001) Random graphs with arbitrary degree distributions and their applications. *Phys Rev E* 64(2):026118
- Pósfai M, Barabási A-L (2016) *Network science*. Cambridge University Press, Cambridge, UK
- Redner Sidney (2019) Reality-inspired voter models: a mini-review. *C R Phys* 20(4):275–292
- Ross Sheldon M (2014) *Introduction to probability and statistics for engineers and scientists*, 5th edn. Academic Press, Cambridge
- Shang Yilun (2013) Deffuant model with general opinion distributions: first impression and critical confidence bound. *Complexity* 19(2):38–49
- Shang Yilun (2018) Hybrid consensus for averager–copier–voter networks with non-rational agents. *Chaos Solitons Fractals* 110:244–251
- Shao J, Havlin S, Stanley HE (2009) Dynamic opinion model and invasion percolation. *Phys Rev Lett* 103(1):018701
- Sun X, Kaur J, Milojević S, Flammini A, Menczer F (2013) Social dynamics of science. *Sci Rep* 3(1):1–6
- Sznajd-Weron K, Sznajd J (2000) Opinion evolution in closed community. *Int J Mod Phys C* 11(06):1157–1165
- Sznajd-Weron K (2005) Sznajd model and its applications. *arXiv preprint physics/0503239*
- Sírbu A, Loreto V, Servedio VDP, Triá F (2016) Opinion dynamics: models, extensions and external effects. In: Loreto V et al (eds) *Participatory sensing, opinions and collective awareness. Understanding Complex Systems*. Springer, Cham, pp 363–401
- Van Mieghem P (2014) *Performance analysis of complex networks and systems*. Cambridge University Press, Cambridge
- Walker Helen M, Helen M (1985) De Moivre on the law of normal probability. In: Smith, David Eugene. *A Source Book in Mathematics*, Dover, pp 64690–64694

Publisher's Note

Springer Nature remains neutral with regard to jurisdictional claims in published maps and institutional affiliations.